# Alteration of χ recognition by RecBCD reveals a regulated molecular latch and suggests a channel-bypass mechanism for biological control

Liang Yang[a,1], Naofumi Handa[a,b,1], Bian Liu[a], Mark S. Dillingham[c], Dale B. Wigley[d], and Stephen C. Kowalczykowski[a,2]

[a]Department of Microbiology and Department of Molecular and Cellular Biology, University of California, Davis, CA 95616; [b]Department of Medical Genome Sciences, Graduate School of Frontier Sciences, University of Tokyo, Shirokanedai, Minato-ku, Tokyo 108-8639, Japan; [c]DNA-Protein Interactions Unit, School of Biochemistry, University of Bristol, Bristol BS8 1TD, United Kingdom; and [d]Division of Structural Biology, Chester Beatty Laboratories, Institute of Cancer Research, London SW3 6JB, United Kingdom

Contributed by Stephen C. Kowalczykowski, April 12, 2012 (sent for review February 21, 2012)

**The RecBCD enzyme is a complex heterotrimeric helicase/nuclease that initiates recombination at double-stranded DNA breaks. In *Escherichia coli*, its activities are regulated by the octameric recombination hotspot, χ (5′-GCTGGTGG), which is read as a single-stranded DNA sequence while the enzyme is unwinding DNA at over ∼1,000 bp/s. Previous studies implicated the RecC subunit as the "χ-scanning element" in this process. Site-directed mutagenesis and phenotypic analyses identified residues in RecC responsible for χ recognition [Handa N, et al., (2012) *Proc Natl Acad Sci USA*, 10.1073/pnas.1206076109]. The genetic analyses revealed two classes of mutants. Here we use ensemble and single-molecule criteria to biochemically establish that one class of mutants (type 1) has lost the capacity to recognize χ (lost-recognition), whereas the second class (type 2) has a lowered specificity for recognition (relaxed-specificity). The relaxed-specificity mutants still recognize canonical χ, but they have gained the capacity to precociously recognize single-nucleotide variants of χ. Based on the RecBCD structure, these mutant classes define an α-helix responsible for χ recognition that is allosterically coupled to a structural latch. When opened, we propose that the latch permits access to an alternative exit channel for the single-stranded DNA downstream of χ, thereby avoiding degradation by the nuclease domain. These findings provide a unique perspective into the mechanism by which recognition of a single-stranded DNA sequence switches the translocating RecBCD from a destructive nuclease to a constructive component of recombinational DNA repair.**

protein–DNA interactions | allosteric switch

In *Escherichia coli*, homologous recombination is initiated by the RecBCD enzyme (1). RecBCD is a helicase/nuclease that processes linear double-stranded DNA (dsDNA) resulting from dsDNA breaks (2) to produce single-stranded DNA (ssDNA) onto which it loads the RecA protein (3). These RecA-ssDNA filaments are essential to the formation of homologously paired joint molecules that are intermediates of recombinational DNA-break repair.

RecBCD binds to dsDNA ends with high affinity ($K_M \sim 0.1$–1 nM) (4, 5). It is a rapid and highly processive helicase, unwinding DNA at up to 1,000–1,500 bp/s, translocating about 30,000 bp before dissociating, and using ∼2 ATP molecules per base pair unwound (4–6). The RecBCD enzyme is driven by two motor subunits, RecB and RecD, with opposite translocation polarities, 3′ →5′ and 5′ →3′, respectively (7, 8). As it is unwinding, RecBCD degrades the nascent ssDNA, preferentially on the 3′-teminated strand relative to its DNA entry site (9).

RecBCD is regulated by the recombination hotspot, χ, the octameric DNA sequence (5′-GCTGGTGG-3′) (10), which is recognized from its 3′-side as ssDNA by the translocating enzyme (9, 11, 12). In response to χ recognition, the polarity of RecBCD nucleolytic action is switched: degradation of the 3′-terminated strand is down-regulated, whereas degradation of the 5′-terminated strand is up-regulated (9, 13, 14). Upon interaction with χ, RecBCD also briefly pauses and then resumes translocation, but at approximately half the initial rate (15–17). Because the helicase activity is retained (9), ssDNA is produced with χ at its 3′-terminus, which is the optimal substrate for RecA-promoted invasion of dsDNA (14). Thus, interaction with χ changes RecBCD from its "destructive" mode, digesting DNA as it unwinds, to a "recombinational" mode, preserving the χ-containing ssDNA and loading RecA onto this ssDNA (1, 2); these are two essential biological functions of the RecBCD–χ interaction (18, 19).

The crystal structure of RecBCD bound to a DNA hairpin provided a great deal of information in understanding RecBCD function, in particular with regard to the potential role of RecC in χ recognition (20). Strikingly, RecC displays the fold of a canonical UvrD-like helicase, even though none of the characteristic Superfamily 1 (SF1) helicase motifs are preserved. There are three holes in RecC: a large one flanked by two smaller ones. The large hole serves as the interface between the RecB and RecC subunits. One of the small tunnels feeds the 5′-terminated ssDNA strand to RecD, and the other feeds the 3′-terminated strand from RecB, through RecC, into a nuclease domain immediately "behind" the RecB motor domains. The 3′-strand tunnel in RecC is formed by the helicase-like domains, and the *recC** mutants, which alter the efficiency and specificity of χ recognition, map to this region (21–23). Consequently, it was proposed that this tunnel region functions to channel a correctly oriented χ sequence for recognition by RecC.

In the companion article by Handa et al. (24), amino acids within the RecC channel were altered by site-directed mutagenesis to identify the residues responsible for χ recognition. The genetic analyses discovered two types of mutants (Fig. S1). The first category, referred to as type 1, displayed phenotypic characteristics consistent with a complete loss of the χ response; these mutants included L64A, W70A, D133A, D136A, and R186A, and recombination in these cells was not responsive to χ. In contrast, the second category, referred to as type 2, displayed phenotypic characteristics consistent with a promiscuous response to χ: these mutants included Q38A, T40A, L134A, Q137A, R142A, and D705A. To understand the biochemical basis for these complex phenotypes in vivo, six mutant proteins of each type were purified and their in vitro behavior was investigated. We found that the type 1 mutants represent a group of RecBCD enzymes that fail to recognize χ, and that the type 2 mutants

Author contributions: L.Y., N.H., M.S.D., D.B.W., and S.C.K. designed research; L.Y., N.H., and B.L. performed research; L.Y., N.H., and B.L. contributed new reagents/analytic tools; L.Y., N.H., B.L., M.S.D., D.B.W., and S.C.K. analyzed data; and L.Y., N.H., B.L., M.S.D., D.B.W., and S.C.K. wrote the paper.

The authors declare no conflict of interest.

[1]L.Y. and N.H. contributed equally to this work.

[2]To whom correspondence should be addressed. E-mail: sckowalczykowski@ucdavis.edu.

This article contains supporting information online at www.pnas.org/lookup/suppl/doi:10.1073/pnas.1206081109/-/DCSupplemental.

represent a group that displays relaxed recognition specificity toward χ. The members of the first group define a recognition helix structure for sequence-specific binding of ssDNA. The members of the second group define an ionic latch structure associated with the recognition helix. Our findings suggest that the latch is a χ-regulated structure responsible for controlling a conformational switch that, we propose, opens a "trap door" to provide a new exit channel for the χ-containing ssDNA, thereby avoiding nucleolytic degradation. Thus, χ recognition initiates a conformational cascade in RecBCD that transforms its biological behavior by a unique mechanism that acts to divert ssDNA to an alternative exit, thereby escaping nucleolytic demise.

## Results

**RecC-Channel Mutants Possess Approximately Wild-Type Levels of Helicase and Nuclease Activities.** The core activities, dsDNA unwinding and nuclease, of the RecBCD mutants were examined; wild-type RecBCD and RecBC (which lacks nuclease activity) were used as the reference enzymes. All of the mutant enzymes catalyzed unwinding of linear dsDNA, seen as disappearance of substrate and appearance of full-length ssDNA (Fig. S2). The mutants also possessed nuclease activity, which was manifest as production of random-sized oligomeric ssDNA and, because of the heterogeneous sizes, apparent loss of DNA. Because the nuclease activity of RecBCD is significantly affected by the free $Mg^{2+}$ concentration (25), the mutants were also examined at a higher concentration of $Mg^{2+}$ (Fig. S3). At these conditions, nuclease activity was higher, yielding lower amounts of full-length ssDNA. Thus, the relative unwinding and degradative activities of the mutant enzymes were comparable to wild-type, except for W70A, which produced ~twofold more full-length ssDNA, and L64A, which produced approximately half of the full-length ssDNA. However, in comparison with the nuclease-deficient RecBC, all of the mutant enzymes display significant levels of nuclease activity.

**Type 1 Mutants Produce Trace Amounts of χ-Containing ssDNA, Demonstrating a Loss of χ Response.** To determine whether the RecC-channel mutant enzymes respond to χ, we measured production of χ-specific ssDNA as a consequence of χ-dependent attenuation of nuclease activity (9). As previously reported, unwinding and degradation of χ-containing dsDNA by the wild-type RecBCD resulted in formation of full-length ssDNA and χ-specific ssDNA fragments (9, 14, 25). RecBCD converted 40 ± 4% of the dsDNA into $\chi^3$-containing ssDNA (Fig. 1). In contrast, type 1 mutants (L64A, W70A, D133A, D136A, and R186A) generated barely detectable amounts: only 0.2–2%. Experiments at the higher free-magnesium concentration (Fig. S4) showed that yields of $\chi^3$-containing ssDNA were lower (undetectable to 0.5%), but relative behavior was the same. Thus, consistent with their phenotypes, these mutant enzymes lost the ability either to recognize or to be regulated by χ. The inability of type 1 mutants to produce χ-containing ssDNA establishes their designation as "lost-recognition" mutants, a description that we use interchangeably hereafter.

**Type 1 Mutants Have Lost the Ability to Recognize χ.** The lost-recognition mutants failed to either recognize χ or attenuate their nuclease activity in response to χ. To distinguish between these possibilities, we used an assay, reversible inactivation by χ, which is independent of nuclease activity (19, 26). Under conditions of limited $Mg^{2+}$, RecBCD is stably but reversibly inactivated after an encounter with χ. The enzyme completes unwinding of the DNA molecule to which it is bound, but the inactivated RecBCD is incapable of reinitiating unwinding on a new DNA duplex. However, inactivation is reversed by addition of excess $Mg^{2+}$, and normal catalytic DNA processing activities are restored to the reactivated enzyme.

This behavior is shown in Fig. 2. Reactions contained subsaturating amounts of enzyme and either $\chi^0$ (Fig. 2*A*) or $\chi^3$ linear

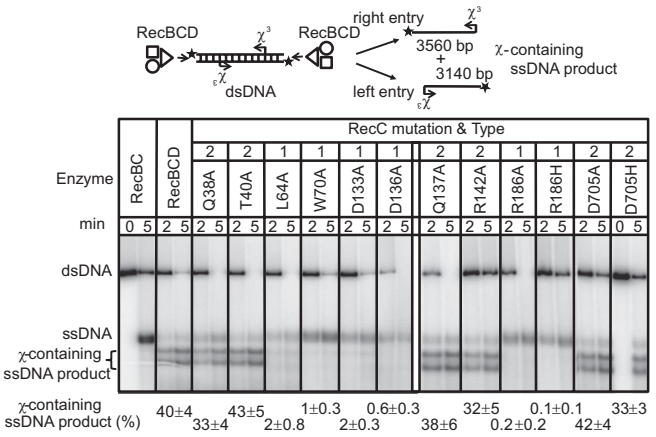


**Fig. 1.** Type 1 (lost-recognition) mutants process dsDNA to produce negligible amounts of χ-specific ssDNA, whereas type 2 (relaxed-specificity) mutants display wild-type levels of χ recognition. Enzymes and reaction times are indicated. The substrate was $\chi^3$ dsDNA [illustrated; processing produces ssDNA and χ-specific ssDNA fragments (only the χ-containing ssDNA product is shown)]. Final yields (± SD) of χ-containing ssDNA product are from at least three independent experiments.

dsDNA (Fig. 2*B*). At the limiting $Mg^{2+}$ concentration, wild-type RecBCD unwound ~60% of $\chi^0$ dsDNA after 20 min, and nearly all (~80%) by 40 min; however, for $\chi^3$ DNA, only 25% was unwound after 20 min and no further unwinding occurred. The reversibility of this phenomenon was demonstrated by the subsequent unwinding of remaining DNA upon increasing the $Mg^{2+}$ concentration. In contrast, the behavior of all lost-recognition mutants on either $\chi^0$ or $\chi^3$ DNA was the same: there was no recognition of χ.

**Lost-Recognition Mutants Do Not Promote χ-Dependent Joint Molecule Formation.** For wild-type RecBCD, interaction with χ not only produces χ-containing ssDNA but results in the preferential loading of RecA onto this product (3). To verify that RecA did not alter our in vitro results, a coupled DNA unwinding and pairing assay was used. In this reaction, RecBCD generates ssDNA, which can be coated by RecA; the resultant RecA nucleoprotein filament invades homologous supercoiled DNA, leading to the formation of joint molecules (Fig. 3). Two types of discrete-sized joint molecules are produced: χ-independent, because of invasion by full-length ssDNA, and χ-dependent, because of invasion by χ-containing ssDNA.

As shown in Fig. 3, wild-type RecBCD preferentially loads RecA onto the χ-containing ssDNA, which is manifest as an increased yield of χ-dependent joint molecules relative to the χ-independent joint molecules. Processing by wild-type RecBCD

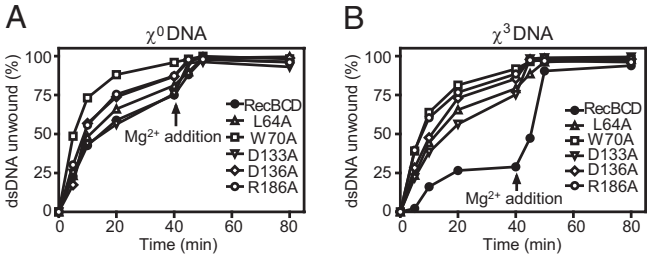


**Fig. 2.** Type 1 (lost-recognition) mutants are not reversibly inactivated by χ. Plotted is dsDNA unwound as a function of time. Reactions contained excess [6.25 μM (nucleotides; 1.55 nM ends)] $\chi^0$ DNA (*A*) or $\chi^3$ DNA (*B*), 0.05 nM RecBCD or equivalent of mutant, 1.25 μM SSB, 1 mM $Mg(OAc)_2$, and 5 mM ATP. At 40 min, $Mg(OAc)_2$ was added to 10 mM.

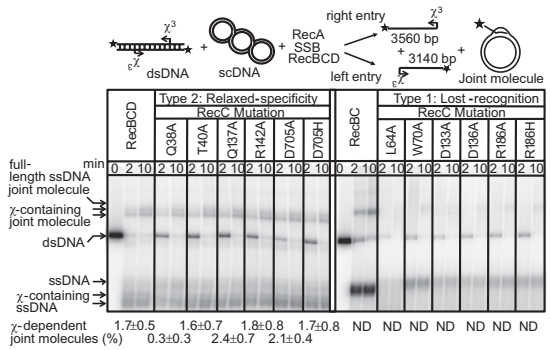


**Fig. 3.** Type 2 (relaxed-specificity) mutants stimulate χ-dependent joint molecule formation, whereas type 1 (lost-recognition) mutants do not. Coupled RecABCD reactions (illustrated) were conducted with enzymes for times indicated. Mobilities of full-length ssDNA, χ-specific ssDNA fragments, and joint molecules are indicated. The final yields (± SD) of χ-dependent joint molecules are from at least three independent experiments; ND signifies not detectable (<0.2%).

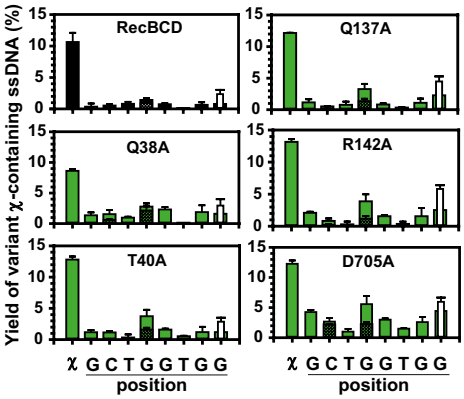


**Fig. 4.** Type 2 (relaxed-specificity) mutants recognize single-base variants of χ. Yield of variant χ-containing ssDNA produced by a mutant enzyme is plotted versus position of the canonical χ sequence. Canonical recognition is the leftmost bar; solid, crosshatched, or white bars denote substitution of adenine, thymine, or cytosine at that position, respectively (Table S1). Final yields (± SD) from at least two independent experiments are plotted. There is only one χ sequence in the proper orientation, and because RecBCD can enter from either DNA end, the efficiency of χ recognition is at least twofold higher.

resulted in ~2% of the input dsDNA substrate being incorporated into $\chi^3$-specific joint molecules. However, the lost-recognition enzymes did not promote any detectable joint molecule formation and did not increase the yield of $\chi^3$-specific ssDNA in the presence of RecA.

**Type 2 Mutants Produce χ-Specific ssDNA Fragments.** In contrast to type 1, type 2 mutants (Q38A, T40A, Q137A, R142A, and D705A) behaved in vivo as though they recognized a more frequent variant of the χ sequence, or they switched to the χ-activated state randomly. Fig. 1 also showed that processing of $\chi^3$-containing dsDNA by type 2 mutants was distinctly different from lost-recognition mutants. The type 2 mutants behaved similarly to wild-type RecBCD: they recognized χ and produced χ-specific ssDNA products with comparable yields (32–43%).

**Type 2 Mutants Stimulate χ-Dependent Joint Molecule Formation.** Type 2 mutant enzymes loaded RecA onto χ-containing ssDNA to produce amounts of χ-specific joint molecules comparable to wild-type RecBCD (Fig. 3). Both wild-type and type 2 mutant enzymes produced ~10-fold more χ-dependent than χ-independent joint molecules. These data demonstrate that the preferential use of χ-containing ssDNA over full-length ssDNA is retained by type 2 mutants. Thus, type 2 mutants not only respond to χ by attenuating their nuclease activity, but also with the structural changes that enable loading of RecA onto χ-containing ssDNA.

**Type 2 Mutations Create RecBCD Mutants with Relaxed-Specificity That Recognize Sequence Variants of χ.** In vivo, type 2 mutants enabled large plaques for both $\chi^0$ and $\chi^+$ phages, and they showed high recombination frequency even for $\chi^0$ phage λ (24). The biochemical data above showed that these mutants recognize and undergo modification of nuclease functions by χ. One possible explanation for their hyper-recombinogenic phenotype is that type 2 mutants acquired the capacity to recognize χ-related sequences other than the canonical χ sequence.

This possibility was tested by using DNA that contained mutant derivatives of the canonical χ sequence, wherein all of the bases of χ were individually altered initially to adenine, and several were changed to thymine or cytosine (Table S1) based on whether they were known to disrupt recognition by wild-type enzyme (27–29). For DNA containing canonical χ, χ-containing ssDNA was produced by wild-type and all type 2 enzymes (Fig. 4, first column in each graph) (9, 14). For wild-type RecBCD, mutation in any position to adenine nearly eliminated χ recognition (7- to 400-fold lower). Interestingly, type 2 mutants responded more promiscuously to the χ variants than wild-type (Fig. 4 and Fig. S5), revealing their behavior as "relaxed-specificity" alterations, a designation that we will use interchangeably with type 2 mutations hereafter. For D705A, recognition of these χ variants is particularly evident: substitution of adenine at any position resulted in downstream χ-variant ssDNA yields as large as ~25% of the canonical χ response, and recognition of every χ variant was ~2- to 60-fold greater than for wild-type RecBCD (Fig. S5). The Q38A, T40A, Q137A, and R142A enzymes recognized the same χ variants, with only somewhat lower yields (Fig. 4 and Fig. S5).

**Single-Molecule Visualization Shows That Translocation by a Relaxed-Specificity Mutant is Modified by χ-Like Sequences in a Canonical Manner.** Interaction with χ not only alters the intensity and polarity of the nuclease activity, but it also changes translocation: upon recognition of χ, RecBCD pauses and then continues at approximately one-half of the initial rate (15, 16). Consequently, we were interested in determining whether χ-like sequences behaved as bona fide χ sequences with regard to translocation by relaxed-specificity mutants. The single-molecule approach described (15, 17, 30) was used to directly image translocation of the most promiscuous relaxed-specificity mutant, RecBC(D705A)D. Wild-type λ DNA does not have a canonical χ sequence but, when attached via its *cosA* end to polystyrene beads, it does contain potential χ variants in the correct orientation relative to the *cosB* end (Fig. 5*A*, arrows).

For wild-type RecBCD, unwinding and degradation was linear with time, with neither pauses nor changes in velocity (Table S2) (15, 17, 30). The average rate of unwinding for 24 RecBCD molecules was comprised of two Gaussian populations with mean velocities of 861 ± 99 bp/s and 368 ± 191 bp/s (at 29 °C), and is consistent with earlier measurements (4, 15, 30); the slower population (~20%), which becomes evident when a large number of molecules was sampled, will not be discussed further herein (31). In contrast, Fig. 5*A* shows three examples of RecBC(D705A)D translocating on λ DNA lacking the canonical χ sequence. These three enzyme molecules paused and altered velocity; furthermore, they paused at different positions. Out of the 56 RecBC(D705A)D–DNA complexes that were trapped, 23 (41%) of the mutant enzymes were seen to pause (Table S3). In contrast, none of the 24 wild-type enzymes paused. Before pausing, the collection of RecBC(D705A)D molecules displayed a translocation velocity distribution that is nearly the same as wild-

BIOCHEMISTRY

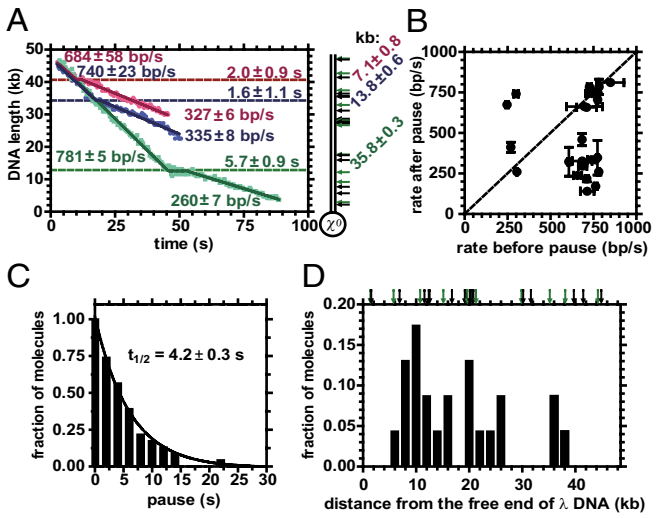


**Fig. 5.** Single-molecule visualization shows that translocation by RecBC(D705A)D is modified by encounters with sequences that elicit a χ-like response. (*A*) Time course for unwinding of three different λ DNA molecules, which lack canonical χ, by individual RecBC(D705A)D enzymes at 29 °C. For each, velocity before and after a pause, pause position, and pause duration are indicated. Arrows represent positions of single-base χ variants; green arrows are variants examined biochemically in Fig. 4 (see *SI Materials and Methods* for sequences and locations). (*B*) Dot plot for rate of translocation before pausing versus after pausing. Diagonal line denotes expectation if the rates were identical. Error bars are SEs. (*C*) Distribution of pause times. Molecules that paused for at least the time indicated were grouped in 2-s bins. The half-time for decay is 4.2 ± 0.3 s. (*D*) Positions where RecBC(D705A)D paused. Arrows are as in *A*.

type enzyme (710 ± 51 bp/s and 284 ± 44 bp/s) (Fig. S6), within error, verifying that helicase activity is not altered by the D705A mutation. For the 23 RecBC(D705A)D molecules that paused, 17 molecules (74%) changed their translocation velocity (Fig. 5*B*) (15). For each molecule, the translocation velocity after the pause was constant. Most of the 23 molecules slowed after the pause, except for six enzymes that maintained the same speed and another four that increased velocity, a behavior that can also be observed for wild-type RecBCD (31). The pauses have a half-time of 4.2 ± 0.3 s (Fig. 5*C*), which is similar (within error) to the half-time (5.0 ± 0.5 s) for wild-type RecBCD elicited by the canonical χ (15).

Although wild-type λ DNA does not have a canonical χ sequence, it does have 27 singe-base variants of χ (Fig. 5*D*, arrows), a subset of which were biochemically examined in Fig. 4 (green arrows). Individual RecBC(D705A)D enzymes were seen to pause at many different positions in the λ DNA, ranging from 6 to 38 kb from the free end (Fig. 5*D*). The spatial resolution of our method does not permit precise mapping of these pause sites, but it is clear that they do not always coincide with any arrows (i.e., variants containing seven of eight bases), suggesting that other novel sequences are being recognized. Furthermore, the observed recognition frequency decreases with distance from the entry site; this phenomenon is consistent with a χ-like behavior because RecBCD is switched at the first productive encounter with χ, and it does not respond to subsequent downstream χ sequences (15, 32). It is clear that the most promiscuous of the relaxed-specificity mutants is responding to many different χ-like sequences in a way that is identical to the behavior induced upon recognition of χ by wild-type RecBCD. Thus, the interaction with χ variants not only modifies the nuclease activities of RecBC(D705A)D, but it also modifies its translocation behavior.

## Discussion

To understand the mechanism by which RecBCD is regulated by its interaction with χ, structure-directed mutagenesis was used to alter residues in the channel of RecC through which the χ-containing ssDNA traverses (24). Based on phenotype, these RecC-channel mutants were classified into two categories: type 1 [L64A, W70A, D133A, D136A, and R186A (or R186H)], and type 2 [Q38A, T40A, L134A, Q137A, R142A, and D705A (or D705H)]. Their in vivo behavior suggested that the first class represented mutants that lost the ability to recognize or respond to χ, and the second class likely represented mutants that gained the ability to respond to more frequent χ-like sequences. Here we established, based on biochemical and single-molecule criteria, that type 1 mutations produce enzymes unable to recognize χ, and that type 2 mutations relax the sequence specificity of χ recognition. All mutant enzymes possess helicase and nuclease activities; when normalized for specific helicase activity (4), their nuclease activities are similar (within ~twofold) to wild-type levels.

The lost-recognition mutants lose the ability to respond to χ and they produce negligible amounts of χ-containing ssDNA. The collective lack of χ response is most consistent with a deficiency in the primary event of χ recognition, not just a failure to communicate the recognition to the required structural changes.

In contrast, relaxed-specificity mutants recognize χ, respond appropriately to produce χ-containing ssDNA, and stimulate DNA pairing by loading RecA onto ssDNA in a χ-dependent manner. Most significantly, relaxed-specificity mutant enzymes recognize variants of χ that alter one of the canonical bases, resulting in a χ-like biochemical response with sequences that contain only seven of the eight bases. In addition, the relaxed-specificity D705A mutant shows precocious χ-like behavior at the single-molecule level, emulating the canonical χ-response at many positions on λ DNA. Thus, type 2 mutants have acquired a relaxed and altered χ-recognition capacity, demonstrating that evolution of novel ssDNA sequence recognition requires only simple point mutation. Because wild-type phage λ has many χ variants, even if less efficient than canonical χ, the seven-base variants will be more frequent and both recombination and repair proficiency of $\chi^0$ phage in the relaxed-specificity class of mutant cells is readily understood. Furthermore, frequent recognition of χ variants, particularly before the crossover interval studied in vivo, would preempt any activation by canonical χ, explaining the lack of hotspot activity in the in vivo assays. The relaxed-specificity mutants might also recognize shorter versions (e.g., six nucleotides) of χ; this was not tested here. It is known, for example, that the χ sequence for the *Bacillus subtilis* RecBCD homolog, AddAB, is five nucleotides: 5′-AGCGG-3′ (33).

The ensemble conclusions are also confirmed by single-molecule analyses. Wild-type λ DNA lacks canonical χ but, nonetheless, both a pause and change in translocation rate (characteristic of bona fide χ recognition) occur at different positions for the relaxed-specificity mutant, RecBC(D705A)D. This finding supports the idea that relaxed-specificity mutants do indeed interact with novel sequences, and that translocation is quantitatively modified in the canonical manner upon recognition of non-canonical sequences. The pause positions are not limited to the sites of χ variants examined here biochemically, implying that RecBC(D705A)D, the most relaxed member of this class, responds to additional undefined χ-like sequences.

Structurally, RecC has the same tertiary-fold as canonical UvrD-like helicases (20). UvrD-like enzymes bind ssDNA via aromatic stacking interactions with nucleobases and electrostatic contacts with the phosphate backbone. Remarkably, many residues involved in χ recognition are located in regions of RecC that are equivalent to regions of helicases involved in ssDNA binding (34, 35), supporting the notion that this region in RecC provides an ideal protein architecture to function as a scanning site for a correctly oriented χ sequence (20, 23). One relaxed-specificity residue, D705, is found in subdomain 2A and five

other relaxed-specificity residues (Q38, T40, L134, Q137, and R142) are located in subdomains 1A, 1B, and 2A. Q38 and T40 are in positions where they could contact the ssDNA backbone (Fig. S1). R142 and D705 form an ion pair latch in a loop at the end of a long helix, on which the relaxed-specificity residues (L134 and Q137) and lost-recognition residues (D133 and D136) are located. Disruption of the ion pair by mutation results in a RecBCD that is more easily activated by effector (χ-like) sequences. It might be that when χ is recognized, via both specific and nonspecific interactions, helix movement results in disruption of the ion pair between R142 and D705. This latch disruption and subsequent structural change would allow RecC to adopt a conformation more typical of an SF1 helicase, opening the existing crevice between RecB and RecC to function as an alternative exit channel for ssDNA away from the nuclease site (Fig. 6*A*, magenta tunnel), thereby escaping nucleolytic degradation. The stable binding of χ to RecC would encourage use of this post-χ recognition exit, because the binding would obstruct the normal exit as the RecB motor continues to pump ssDNA into RecC at ~1,000 nt/s (15, 36). Both structural and biochemical work have noted existence of the alternative channel in Fig. 6*A* (20, 37). A conformational change linked to latch disruption would enable this conformational switch. A similar mechanism of signal transduction along a helix connecting two sites was proposed for an allosteric switch in lactate dehydrogenase (38). For lost-recognition RecBCD mutants, the alteration likely weakens direct interactions with χ to the extent that the binding energy is insufficient to trigger subsequent changes needed to open the latch structure.

The crystal structure of RecBCD with the longest DNA substrate showed how the 3′-tail of DNA interacts with RecB; unfortunately, the ssDNA stopped at the boundary between the RecB and RecC subunits (39). However, an examination of RecC reveals that, in its present conformation (the preinitiation complex before χ recognition), the RecC domains equivalent to the 1A, 1B, and 2A domains of RecB, which interact with ssDNA, are not properly oriented to bind ssDNA in the canonical SF1-helicase manner. Therefore, to gain insight into the possible structural changes required for binding, we used the RecB-ssDNA components from the RecBCD complex (Fig. S7*A*) to model the hypothetical orientations of the 1A, 1B, and 2A domains of RecC when bound to ssDNA. This process was done by simply superimposing them onto the $C_\alpha$ backbone of equivalent domains of RecB to place them in orientations equivalent to the ssDNA binding mode of RecB. We then highlighted the mutated side chains of each class to see where they were located relative to the ssDNA in this fitted model; for ssDNA, we used the eight bases of the χ sequence. This crude "model" (Fig. S7*B*) revealed that the lost-recognition mutants were in positions that could interact with the DNA bases themselves and, hence, their interactions with ssDNA would be entirely sequence-dependent (Fig. S7*C*). Consistent with our experimental observations, this structural approximation shows that alteration of these residues could result in the loss of specific interactions that contribute to the free energy of interaction, leading to an expected loss of recognition. The relaxed-specificity mutants were either in positions that could interact with the DNA backbone or were associated with the latch structure. Alteration of some of these resides could lead to interactions that potentially increased nonspecific interactions with ssDNA, and could lead to a heightened overall free energy of interaction with noncanonical χ sequences, stabilizing this proposed post-χ state. Alternatively, and more probably, alteration could weaken the stability of the latch structure (notably, D705A and R142A), permitting the normally weaker interactions with noncanonical χ sequences to trigger opening of the latch at a lower threshold of binding free energy (i.e., at a lower energetic cost). Interestingly, to allow the movement of the domain required for this simple conformational modeling, the latch structure must be disrupted, which is qualitatively consistent with the mutational interpretations and energetic consideration mentioned above. Although this rough model does not provide an explanation for why D705A shows more promiscuous recognition than mutation of its partner, R142, we suspect that mutation on one side of the latch, but not the other, is detrimental to other local contacts in the vicinity. Finally, although this model appears to give some insights into the likely roles of the mutations, it must be stressed that this is only a crude model and merely serves for illustrative purposes to indicate the likely positions of the mutations in the channel and how ssDNA might run past them (Fig. 6*B*). It is certainly too imprecise for any detailed analysis beyond that which we present here.

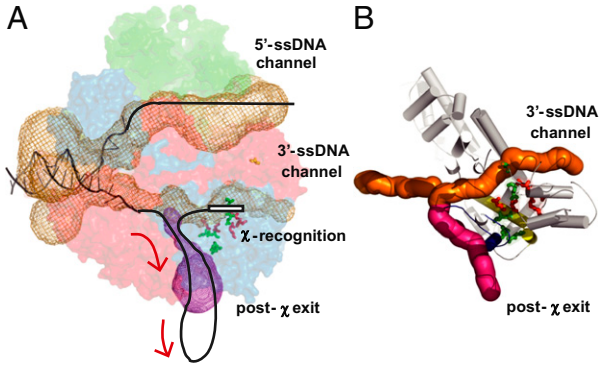


**Fig. 6.** Proposed model for the interaction between RecBCD and χ. (*A*) Location of the χ-binding locus within RecBCD. Red and green residues are type 1 and type 2, respectively. Duplex DNA enters on left and exits at nuclease domain on right. Pre-χ recognition channels are orange; proposed post-χ recognition exit is magenta. The proposed exit path for ssDNA after χ recognition is shown. (*B*) Proposed alternative exit in RecBCD post-χ recognition. Path of ssDNA before χ recognition is in orange; the proposed alternative exit after χ recognition is shown in rose. Recognition helix is yellow and structural elements (blue) comprising the latch line alternative exit.

In summary, our genetic, biochemical, single-molecule, and structural analyses reveal both a complexity and elegance to the manner by which RecBCD is regulated by its interaction with the ssDNA sequence, χ, while it is translocating through duplex DNA, and they suggest a model for how that recognition event is transmitted into both structural and functional alterations. We show that χ is recognized by the RecC subunit while it is being pushed through a channel by the RecB motor (40). The lost-recognition (type 1) mutations define the locus for this interaction, and they define an ssDNA-recognition helix that is needed to confer and communicate the specificity of this interaction. The relaxed-specificity (type 2) mutations define the latch as a crucial structural element. We propose that latch opening is triggered via allosteric coupling with the recognition helix that permits conformation switching to the χ-activated structure. This structure is an engineering masterpiece that couples recognition of χ to movement of an α-helix that then snaps open a latch, which then opens an alternative exit for the χ-containing ssDNA to avoid degradation by the nuclease domain. Mutations that weaken this latch structure or that increase nonspecific interaction with ssDNA, facilitate structural unlatching: thus, evolutionarily, it would be a simple matter to tune in the requisite specificity and stability of sequence-specific ssDNA interaction to evolve proteins with a broad range of χ-sequence interaction. We propose that, as a consequence of structural changes that accompany unlatching of the χ-activated state, the combined nuclease and RecA-loading site of RecBCD is then forced to undock from its interaction site on RecC (15). This structural change is both encouraged and stabilized by the stable binding of χ to RecC in the channel (15, 36). This stable binding both prevents the 3′-end of the χ-containing ssDNA from exiting into the nuclease domain and, because RecB continues to pump ssDNA into the channel

(17), the requirement for an alternative exit is imposed. Furthermore, undocking of the RecB nuclease and loading domain has two consequences: (*i*) an attenuation of nuclease activity overall and specifically preventing degradation of the recombinogenic χ-containing ssDNA at the original 3′-exit location (9), and (*ii*) liberation of the RecB domain responsible for RecA-loading, which is now able to swing on the end of its 70 amino acid tether and finally load RecA onto the χ-containing ssDNA (41). Although elements of this model are conjectural, collectively the existing data underscore an exquisite structural and mechanical coupling in this finely tuned macromolecular machine.

## Materials and Methods

**Proteins and DNA.** Biotinylated RecBCD enzymes with RecC-channel mutations, RecA, and SSB were purified as detailed in the *SI Materials and Methods*. Plasmids pBR322 (wild-type, $\chi^0$), pBR322 $\chi^{(+)-3F3H}$ (referred to as $\chi^3$ throughout) (13), and pBR322 containing the χ-variants (Table S1) were purified by cesium chloride density gradient centrifugation. Plasmid DNA was linearized with NdeI and radioactively labeled at the 5′ end.

**DNA Unwinding, χ-Specific ssDNA Fragment Production, Joint Molecule Formation, Reversible Inactivation, and Single-Molecule Visualization Assays.** The following assays were performed as described previously: DNA unwinding (4), production of χ-specific ssDNA fragments (9, 14), joint molecule formation (3, 9, 14), and reversible inactivation by χ (26). Unless indicated otherwise, reaction conditions were 25 mM Tris acetate (pH 7.5), 2 mM $Mg(OAc)_2$, 1 mM ATP, 1 mM DTT, 10 μM (nucleotides) linear pBR322 dsDNA (2.25-nM ends), and 2 μM SSB at 37 °C. Other than reversible inactivation, assays contained 0.1 nM RecBCD, equivalent concentrations (helicase units) of RecC-channel mutants, or 10 nM RecBC. The reaction products were separated on a 1% (wt/vol) TAE agarose gel at 600 V·h, visualized, and quantified using an Amersham Biosciences Storm 840 PhosphorImager; product formation was normalized for the extent of DNA unwinding.

The translocation on single molecules of λ DNA was visualized as previously described (15, 17, 30, 42). For the single-molecule assays, the reaction conditions were 45 mM $NaHCO_3$ (pH 8.2), 20% (wt/vol) sucrose, 50 mM DTT, 1 mM ATP, 2 mM magnesium acetate, and 20 nM YOYO-1 at 29 °C. Details are provided in *SI Materials and Methods*.

**ACKNOWLEDGMENTS.** This work was supported by the following institutions: grants from the Japan Society for the Promotion of Science Postdoctoral Fellowship for Research Abroad, The Naito Foundation, the Kato Memorial Bioscience Foundation, the Takeda Foundation, the Sumitomo Foundation; Grants-in-Aid for Scientific Research from both the Japan Society for the Promotion of Science and Ministry of Education, Culture, Sports, Science and Technology (to N.H.); a Royal Society and Wellcome Trust grant (to M.S.D.); and National Institutes of Health Grant GM41347 (to S.C.K.).

1. Kowalczykowski SC, Dixon DA, Eggleston AK, Lauder SD, Rehrauer WM (1994) Biochemistry of homologous recombination in *Escherichia coli*. *Microbiol Rev* 58: 401–465.
2. Dillingham MS, Kowalczykowski SC (2008) RecBCD enzyme and the repair of double-stranded DNA breaks. *Microbiol Mol Biol Rev* 72:642–671.
3. Anderson DG, Kowalczykowski SC (1997) The translocating RecBCD enzyme stimulates recombination by directing RecA protein onto ssDNA in a χ-regulated manner. *Cell* 90:77–86.
4. Roman LJ, Kowalczykowski SC (1989) Characterization of the helicase activity of the *Escherichia coli* RecBCD enzyme using a novel helicase assay. *Biochemistry* 28: 2863–2873.
5. Roman LJ, Kowalczykowski SC (1989) Characterization of the adenosinetriphosphatase activity of the *Escherichia coli* RecBCD enzyme: Relationship of ATP hydrolysis to the unwinding of duplex DNA. *Biochemistry* 28:2873–2881.
6. Roman LJ, Eggleston AK, Kowalczykowski SC (1992) Processivity of the DNA helicase activity of *Escherichia coli* recBCD enzyme. *J Biol Chem* 267:4207–4214.
7. Dillingham MS, Spies M, Kowalczykowski SC (2003) RecBCD enzyme is a bipolar DNA helicase. *Nature* 423:893–897.
8. Taylor AF, Smith GR (2003) RecBCD enzyme is a DNA helicase with fast and slow motors of opposite polarity. *Nature* 423:889–893.
9. Dixon DA, Kowalczykowski SC (1993) The recombination hotspot χ is a regulatory sequence that acts by attenuating the nuclease activity of the *E. coli* RecBCD enzyme. *Cell* 73:87–96.
10. Lam ST, Stahl MM, McMilin KD, Stahl FW (1974) Rec-mediated recombinational hot spot activity in bacteriophage lambda. II. A mutation which causes hot spot activity. *Genetics* 77:425–433.
11. Bianco PR, Kowalczykowski SC (1997) The recombination hotspot Chi is recognized by the translocating RecBCD enzyme as the single strand of DNA containing the sequence 5′-GCTGGTGG-3′. *Proc Natl Acad Sci USA* 94:6706–6711.
12. Taylor AF, Schultz DW, Ponticelli AS, Smith GR (1985) RecBC enzyme nicking at Chi sites during DNA unwinding: location and orientation-dependence of the cutting. *Cell* 41:153–163.
13. Anderson DG, Kowalczykowski SC (1997) The recombination hot spot χ is a regulatory element that switches the polarity of DNA degradation by the RecBCD enzyme. *Genes Dev* 11:571–581.
14. Dixon DA, Kowalczykowski SC (1991) Homologous pairing in vitro stimulated by the recombination hotspot, Chi. *Cell* 66:361–371.
15. Spies M, et al. (2003) A molecular throttle: The recombination hotspot χ controls DNA translocation by the RecBCD helicase. *Cell* 114:647–654.
16. Handa N, Bianco PR, Baskin RJ, Kowalczykowski SC (2005) Direct visualization of RecBCD movement reveals cotranslocation of the RecD motor after χ recognition. *Mol Cell* 17:745–750.
17. Spies M, Amitani I, Baskin RJ, Kowalczykowski SC (2007) RecBCD enzyme switches lead motor subunits in response to χ recognition. *Cell* 131:694–705.
18. Arnold DA, Kowalczykowski SC (2000) Facilitated loading of RecA protein is essential to recombination by RecBCD enzyme. *J Biol Chem* 275:12261–12265.
19. Anderson DG, Churchill JJ, Kowalczykowski SC (1999) A single mutation, RecB (D1080A,) eliminates RecA protein loading but not Chi recognition by RecBCD enzyme. *J Biol Chem* 274:27139–27144.
20. Singleton MR, Dillingham MS, Gaudier M, Kowalczykowski SC, Wigley DB (2004) Crystal structure of RecBCD enzyme reveals a machine for processing DNA breaks. *Nature* 432:187–193.
21. Schultz DW, Taylor AF, Smith GR (1983) *Escherichia coli* RecBC pseudorevertants lacking chi recombinational hotspot activity. *J Bacteriol* 155:664–680.
22. Handa N, Ohashi S, Kobayashi I (1997) Clustering of chi sequence in *Escherichia coli* genome. *Microb Comp Genomics* 2:287–298.
23. Arnold DA, Handa N, Kobayashi I, Kowalczykowski SC (2000) A novel, 11 nucleotide variant of χ, χ*: One of a class of sequences defining the *Escherichia coli* recombination hotspot χ. *J Mol Biol* 300:469–479.
24. Handa N, et al. (2012) Molecular determinants responsible for recognition of the single-stranded DNA regulatory sequence, χ, by RecBCD enzyme. *Proc Natl Acad USA* 109:8901–8906.
25. Dixon DA, Kowalczykowski SC (1995) Role of the *Escherichia coli* recombination hotspot, χ, in RecABCD-dependent homologous pairing. *J Biol Chem* 270: 16360–16370.
26. Dixon DA, Churchill JJ, Kowalczykowski SC (1994) Reversible inactivation of the *Escherichia coli* RecBCD enzyme by the recombination hotspot χ in vitro: Evidence for functional inactivation or loss of the RecD subunit. *Proc Natl Acad Sci USA* 91: 2980–2984.
27. Cheng KC, Smith GR (1984) Recombinational hotspot activity of Chi-like sequences. *J Mol Biol* 180:371–377.
28. Cheng KC, Smith GR (1987) Cutting of chi-like sequences by the RecBCD enzyme of *Escherichia coli*. *J Mol Biol* 194:747–750.
29. Schultz DW, Swindle J, Smith GR (1981) Clustering of mutations inactivating a Chi recombinational hotspot. *J Mol Biol* 146:275–286.
30. Bianco PR, et al. (2001) Processive translocation and DNA unwinding by individual RecBCD enzyme molecules. *Nature* 409:374–378.
31. Liu B (2010) Single molecule study on the mechanism of χ-regulation of RecBCD activities. PhD thesis (Univ of California, Davis).
32. Taylor AF, Smith GR (1992) RecBCD enzyme is altered upon cutting DNA at a chi recombination hotspot. *Proc Natl Acad Sci USA* 89:5226–5230.
33. Chédin F, Ehrlich SD, Kowalczykowski SC (2000) The *Bacillus subtilis* AddAB helicase/nuclease is regulated by its cognate Chi sequence in vitro. *J Mol Biol* 298:7–20.
34. Lee JY, Yang W (2006) UvrD helicase unwinds DNA one base pair at a time by a two-part power stroke. *Cell* 127:1349–1360.
35. Velankar SS, Soultanas P, Dillingham MS, Subramanya HS, Wigley DB (1999) Crystal structures of complexes of PcrA DNA helicase with a DNA substrate indicate an inchworm mechanism. *Cell* 97:75–84.
36. Chédin F, Handa N, Dillingham MS, Kowalczykowski SC (2006) The AddAB helicase/nuclease forms a stable complex with its cognate χ sequence during translocation. *J Biol Chem* 281:18610–18617.
37. Wong CJ, Rice RL, Baker NA, Ju T, Lohman TM (2006) Probing 3′-ssDNA loop formation in *E. coli* RecBCD/RecBC-DNA complexes using non-natural DNA: A model for "Chi" recognition complexes. *J Mol Biol* 362:26–43.
38. Iwata S, Kamata K, Yoshida S, Minowa T, Ohta T (1994) T and R states in the crystals of bacterial L-lactate dehydrogenase reveal the mechanism for allosteric control. *Nat Struct Biol* 1:176–185.
39. Saikrishnan K, Griffiths SP, Cook N, Court R, Wigley DB (2008) DNA binding to RecD: Role of the 1B domain in SF1B helicase activity. *EMBO J* 27:2222–2229.
40. Spies M, Dillingham MS, Kowalczykowski SC (2005) Translocation by the RecB motor is an absolute requirement for χ-recognition and RecA protein loading by RecBCD enzyme. *J Biol Chem* 280:37078–37087.
41. Spies M, Kowalczykowski SC (2006) The RecA binding locus of RecBCD is a general domain for recruitment of DNA strand exchange proteins. *Mol Cell* 21:573–580.
42. Amitani I, Liu B, Dombrowski CC, Baskin RJ, Kowalczykowski SC (2010) Watching individual proteins acting on single molecules of DNA. *Methods Enzymol* 472:261–291.

# Supporting Information

## Yang et al. 10.1073/pnas.1206081109

### SI Materials and Methods

**Proteins and Reagents.** Biotinylated RecBCD enzymes with RecC-channel mutations were purified from an *Escherichia coli* strain harboring four plasmids, pMS421 (*lacI*$^q$ spc) (1), pPB700 [(2) (*recB*, amp)], derivatives of pNH336 harboring the RecC-channel mutations (*recC*-channel mutants, cam) (3), and pWKS6 [biotin-*recD* kan; a derivative of pWKS130 (4)] in a Δ*recBCD* background. Cells for producing biotinylated RecBCD enzymes were grown in L broth with selective antibiotics and biotin (113 μM). After addition of 1 mM isopropyl-beta-D-thiogalactopyranoside at an $OD_{600}$ of 0.5–0.6, cells were grown for 3–4 h and then harvested. RecC-channel mutants were purified as previously described (5) up to the Q-Sepharose chromatography step. After dialysis against 0.1 M potassium phosphate (pH 7.2) and 0.15 M NaCl, the pool from the Q-Sepharose column (Amersham-Pharmacia) was applied to an UltraLink Immobilized Monomeric Avidin column (Pierce). Biotinylated RecBCD was eluted with 2 mM D-biotin (Sigma), dialyzed to remove biotin, and then stored in 20 mM Tris-HCl (pH 7.5), 0.1 mM EDTA, 0.1 mM DTT, 100 mM NaCl, and 50% (vol/vol) glycerol (6). The concentrations of the purified RecC-channel mutants were determined using an extinction coefficient of $4.0 \times 10^5$ $M^{-1}{\cdot}cm^{-1}$ at 280 nm (7). The specific activity of each mutant enzyme was based on helicase units (7), and appropriate concentrations of wild-type and mutant enzymes were used in each assay to provide equivalent amounts of DNA unwinding activity. RecBC was expressed without pWKS6 in a Δ*recBCD* background and purified (8). Wild-type RecBCD was purified as described previously (5). *E. coli* SSB and RecA proteins were purified as previously described (9, 10).

Chemicals were of reagent grade. Pyruvate kinase, phosphoenolpyruvate, and ATP were purchased from Sigma. Restriction endonucleases, shrimp alkaline phosphatase, T4 polynucleotide kinase were from New England Biolabs; [γ-$^{32}$P]ATP was from Perkin-Elmer; YOYO-1 was from Molecular Probes Inc. ATP was dissolved as concentrated stock solution at pH 7.5, and its concentration was determined spectrophotometrically using an extinction coefficient of $1.54 \times 10^4$ $M^{-1}{\cdot}cm^{-1}$ at 260 nm.

**DNA Substrates.** The NdeI-linearized pBR322 $\chi^{(+)-3F3H}$ ($\chi^3$) (11) substrate has three tandem χ sequences at either end of the linear double-strand (dsDNA) in the proper orientation for RecBCD enzyme entering from that end. Plasmids pNH92, pNH868, pNH869, pNH1556, pNH870, pNH871, pNH872, pNH873, pNH874, pNH875, pNH94, and pNH95, are pBR322 derivatives containing either χ or a variant χ sequence (12), flanked by BamHI and HindIII sites (Table S1). Plasmid DNA was linearized with NdeI or AvaI, and radioactively labeled at the 5′ end by reaction with shrimp alkaline phosphatase, and then with T4 polynucleotide kinase and [γ-$^{32}$P] ATP. Excess [γ-$^{32}$P] ATP was removed using a G-25 or S-200 spin column (GE Healthcare). The dsDNA concentration (nucleotides) was determined using a molar extinction coefficient of 6,290 $M^{-1}{\cdot}cm^{-1}$ at 260 nm.

**DNA Unwinding Assay.** Assays were performed as described previously (7, 13). The reaction mixtures contained 25 mM Tris acetate (pH 7.5), 2 magnesium acetate, 1 mM DTT, 10 μM (nucleotides) linear pBR322 dsDNA $^{32}$P-labeled at the 5′-ends (2.25 nM ends), 1 mM ATP, and 2 μM SSB protein. DNA unwinding reactions were started with the addition of 0.1 nM RecBCD, 10 nM RecBC, or equivalent (in terms of helicase units) concentrations of RecC-channel mutants (0.5 nM Q38A, 0.3 nM T40A, 0.2 nM L64A, 0.5 nM W70A, 0.3 nM D133A, 0.2 nM D136A, 0.4 nM Q137A, 0.5 nM R142A, 0.4 nM R186A, 0.4 nM R186H, 0.3 nM D705A, and 0.4 nM D705H), after preincubation of all other components at 37 °C for 5 min. Assays were stopped at the indicated times by addition of proteinase K to a concentration of 0.5 mg/mL, which was dissolved in 5× sample loading buffer [250 mM EDTA, 2.5% (wt/vol) SDS, and 0.25% (wt/vol) Bromophenol blue]. After a 5-min incubation with proteinase K at 37 °C the reaction products were separated on a 1% (wt/vol) TAE agarose gel at 600 V·h, visualized, and quantified using an Amersham Biosciences Storm 840 PhosphorImager and ImageQuant software.

**χ-Specific Single-Stranded DNA Fragment Production Assay.** Assays were performed as described previously (5, 14–16). The reaction mixtures contained 25 mM Tris acetate (pH 7.5), 1 mM DTT, 10 μM (nucleotides) linear NdeI-linearized or AvaI-linearized pBR322 dsDNA ($\chi^3$, or a single variant-χ) that was $^{32}$P-labeled at the 5′-ends (2.25 nM ends), 2 μM SSB protein, and the indicated concentrations of magnesium acetate and ATP. DNA unwinding reactions were started with the addition of 0.1 nM of RecBCD enzyme, 10 nM RecBC enzyme, or equivalent concentrations of RecC-channel mutants (same as for the DNA unwinding assays), after preincubation of all other components at 37 °C for 5 min. Reactions were stopped, loaded on a 1% (wt/vol) agarose and analyzed as described above for the DNA unwinding assay.

**Joint Molecule Formation Assay.** Coupled RecABCD reactions were performed as described previously (17). The reactions contained 25 mM Tris acetate (pH 7.5), 6 mM magnesium acetate, 2 mM ATP, 1 mM DTT, 1 mM phosphoenolpyruvate, 4 Units/mL pyruvate kinase, 2 μM SSB protein, and 10 μM (nucleotides) of NdeI-linearized, 5′-end-labeled dsDNA ($\chi^3$). In addition, 20 μM (nucleotides) supercoiled pBR322 DNA and 5 μM RecA were included before preincubation at 37 °C. The reactions were initiated with 0.1 nM RecBCD, 10 nM RecBC or equivalent amounts of the RecC-channel mutants (same as for the DNA unwinding assays). Reactions were stopped, loaded on a 1% (wt/vol) agarose, and analyzed as described above for the DNA unwinding assay. The yield of joint molecules formation was determined from the percentage of discrete joint molecules produced relative to the input dsDNA.

**Reversible Inactivation Assay.** Assays were performed as described previously (14, 15, 18). Initial reaction conditions contained 25 mM Tris acetate (pH 7.5), 1 mM magnesium acetate, 5 mM ATP, 1 mM DTT, 6.25 μM plasmid DNA ($\chi^0$ or $\chi^3$, 1.55 nM dsDNA ends), and 1.25 μM SSB protein. After equilibration for 2 min at 37 °C, reactions were initiated by addition of 0.05 nM RecBCD or the equivalent amount of RecC-channel mutant enzyme, and time points were taken as indicated. After 40 min, magnesium acetate was added to 10 mM final concentration, and the time course was continued for an additional 40 min. Reactions were stopped, loaded on a 1% agarose, and analyzed as described above for the DNA unwinding assay. Quantification of duplex DNA remaining was normalized to the amount present at the start of the reaction.

**Single-Molecule Visualization.** The DNA bead preparations and reactions were performed as previously described (19–22). The *cosA* end of λ DNA was attached to beads via a biotinylated oligonucleotide (5′-GGGCGGCGACCT-biotin-3′) that was ligated to the λ DNA using modification of a procedure used

previously (19). The biotinylated DNA (1–5 femtomoles) was incubated with 1–2 μL of 1 μm ProActive streptavidin-coated microspheres (Bangs Laboratories) for 1 h at 37 °C in 80 mM $NaHCO_3$ (pH 8.2). Bead-DNA complexes were transferred into 0.5 mL of degassed sample solution containing 45 mM $NaHCO_3$ (pH 8.2), 20% (wt/vol) sucrose, 50 mM DTT, and 20 nM YOYO-1 dye (Molecular Probes). DNA was incubated with the dye for at least 1 h in the dark at room temperature. Immediately before transfer to the sample syringe, 2 mM magnesium acetate, 8 nM RecBCD enzyme, or 24 nM of RecBC(D705A)D mutant enzyme, were added to the sample mixture. The reaction solution contained 45 mM NaHCO3 (pH 8.2), 20% (wt/vol) sucrose, 50 mM DTT, 1 mM ATP, 2 mM magnesium acetate, and 20 nM YOYO-1 at 29 °C.

Videos of the enzyme translocation were recorded at 5.3 frames per second with Andor iQ (Andor) software. Every two frames were averaged using an ImageJ plug-in to reduce background and to create movies at 2.65 frames per second. The length of the DNA molecule in each frame was measured with a plug-in written in this laboratory (22). The unwinding rates are the best fit values for the slopes of DNA unwinding ± SE obtained from the regression analysis to a contiguous three-segment line using GraphPad Prism Software v4. Values for the extent of DNA unwinding are the difference between the initial length of the DNA molecule and its final length after unwinding. Rates before and after a pause are the best fit values for the slopes of DNA unwinding ± SE obtained from the regression analysis. The average extent of unwinding, $n$, is calculated as follows. The number of enzymes ($Y$) that unwound at least a given DNA length (grouped in 2-kb bins) was plotted against that length ($X$). Processivity, $P$, was determined by fitting the data to the equation $Y = A \times P^X$. The value of $N$ was obtained from $P$ by the equation $N = 1/(1 - P)$ (20). $N$ is reported as the mean ± SE.

Values for the position of the pause are the average length of the DNA molecule measured for each video frame during the appropriate reaction stage ± SE for the DNA lengths measured during this stage. SE for each pause position was calculated using following formula: $SE\ of\ pause\ position = \sqrt{(SE\ of\ intercept1)^2 + (slope1 \times SE\ of\ t1)^2 + (t1 \times SE\ of\ slope1)^2}$, where $t1$ is the beginning of the pause, $intercept1$ is the intercept of the Y/DNA length axis with the unwinding segments before pausing, and $slope1$ is the unwinding rate before pause. The duration of the pause was calculated by subtracting the time when the pause began from the time when the pause ended. SE for the duration of each pause was calculated using following formula:

$SE\ of\ pause\ duration = \sqrt{(SE\ of\ t1)^2 + (SE\ of\ t2)^2}$, where $t1$ and $t2$ are the beginning and the end of the pause.

The sequence and position of single-base variants of χ (arrows in Fig. 5 *A* and *D*) in λ DNA, relative to the cosB entry site, are: *ACTGGTGG* (20,248 bp), G**A**TGGTGG (31,046 bp, 19,857 bp), G**G**TGGTGG (46,285 bp, 32,585 bp), *GC**A**GGTGG* (36,298 bp), GC**C**GGTGG (12,883 bp, 7,069 bp), *GCTGATGG* (39,319 bp, 30783 bp, 15,596 bp, 11,158 bp), GCTG**T**TGG (20,870 bp, 20,764 bp), GCTG**C**TGG (12,035 bp), *GCTGGAGG* (5,877 bp, 1,516 bp), GCTGG**C**GG (21,405 bp, 21,141 bp, 20,116 bp, 17,362 bp, 1,559 bp), *GCTGGTAG* (45,696 bp), GCTGGT**T**G (42,857 bp, 40,948 bp, 12,832 bp), and *GCTGGTGC* (21,835 bp); the variants examined biochemically in Fig. 4 (green arrows in Fig. 5 *A* and *D*) are italicized.


1. Heath JD, Weinstock GM (1991) Tandem duplications of the lac region of the *Escherichia coli* chromosome. *Biochimie* 73:343–352.
2. Boehmer PE, Emmerson PT (1991) *Escherichia coli* RecBCD enzyme: Inducible overproduction and reconstitution of the ATP-dependent deoxyribonuclease from purified subunits. *Gene* 102:1–6.
3. Handa N, et al. (2012) Molecular determinants responsible for recognition of the single-stranded DNA regulatory sequence, χ, by RecBCD enzyme. *Proc Natl Acad USA*, 10.1073/pnas.1206076109.
4. Wang RF, Kushner SR (1991) Construction of versatile low-copy-number vectors for cloning, sequencing and gene expression in *Escherichia coli*. *Gene* 100:195–199.
5. Bianco PR, Kowalczykowski SC (1997) The recombination hotspot Chi is recognized by the translocating RecBCD enzyme as the single strand of DNA containing the sequence 5′-GCTGGTGG-3′. *Proc Natl Acad Sci USA* 94:6706–6711.
6. Handa N, Bianco PR, Baskin RJ, Kowalczykowski SC (2005) Direct visualization of RecBCD movement reveals cotranslocation of the RecD motor after χ recognition. *Mol Cell* 17:745–750.
7. Roman LJ, Kowalczykowski SC (1989) Characterization of the helicase activity of the *Escherichia coli* RecBCD enzyme using a novel helicase assay. *Biochemistry* 28: 2863–2873.
8. Dillingham MS, Spies M, Kowalczykowski SC (2003) RecBCD enzyme is a bipolar DNA helicase. *Nature* 423:893–897.
9. Mirshad JK, Kowalczykowski SC (2003) Biochemical characterization of a mutant RecA protein altered in DNA-binding loop 1. *Biochemistry* 42:5945–5954.
10. LeBowitz JH (1985) Biochemical mechanism of strand initiation in bacteriophage lambda DNA replication. PhD thesis (The Johns Hopkins Univ, Baltimore).
11. Anderson DG, Kowalczykowski SC (1997) The recombination hot spot χ is a regulatory element that switches the polarity of DNA degradation by the RecBCD enzyme. *Genes Dev* 11:571–581.
12. Arnold DA, Handa N, Kobayashi I, Kowalczykowski SC (2000) A novel, 11 nucleotide variant of χ, χ*: One of a class of sequences defining the *Escherichia coli* recombination hotspot χ. *J Mol Biol* 300:469–479.
13. Arnold DA, Bianco PR, Kowalczykowski SC (1998) The reduced levels of χ recognition exhibited by the $RecBC^{1004}D$ enzyme reflect its recombination defect in vivo. *J Biol Chem* 273:16476–16486.
14. Dixon DA, Kowalczykowski SC (1991) Homologous pairing in vitro stimulated by the recombination hotspot, Chi. *Cell* 66:361–371.
15. Dixon DA, Kowalczykowski SC (1993) The recombination hotspot χ is a regulatory sequence that acts by attenuating the nuclease activity of the *E. coli* RecBCD enzyme. *Cell* 73:87–96.
16. Spies M, Dillingham MS, Kowalczykowski SC (2005) Translocation by the RecB motor is an absolute requirement for χ-recognition and RecA protein loading by RecBCD enzyme. *J Biol Chem* 280:37078–37087.
17. Anderson DG, Kowalczykowski SC (1997) The translocating RecBCD enzyme stimulates recombination by directing RecA protein onto ssDNA in a χ-regulated manner. *Cell* 90:77–86.
18. Dixon DA, Churchill JJ, Kowalczykowski SC (1994) Reversible inactivation of the *Escherichia coli* RecBCD enzyme by the recombination hotspot χ in vitro: Evidence for functional inactivation or loss of the RecD subunit. *Proc Natl Acad Sci USA* 91:2980–2984.
19. Bianco PR, et al. (2001) Processive translocation and DNA unwinding by individual RecBCD enzyme molecules. *Nature* 409:374–378.
20. Spies M, Amitani I, Baskin RJ, Kowalczykowski SC (2007) RecBCD enzyme switches lead motor subunits in response to χ recognition. *Cell* 131:694–705.
21. Spies M, et al. (2003) A molecular throttle: The recombination hotspot χ controls DNA translocation by the RecBCD helicase. *Cell* 114:647–654.
22. Amitani I, Liu B, Dombrowski CC, Baskin RJ, Kowalczykowski SC (2010) Watching individual proteins acting on single molecules of DNA. *Methods Enzymol* 472: 261–291.

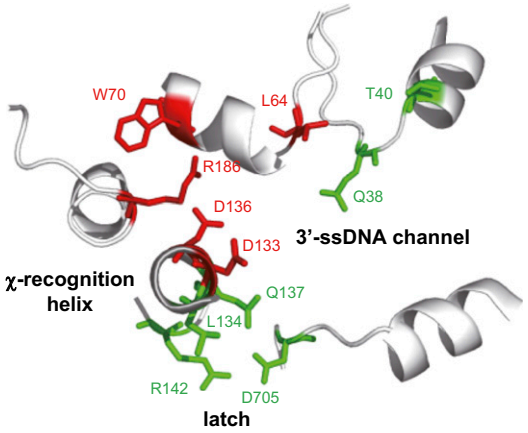


**Fig. S1.** Structural elements from the RecC channel showing the χ-recognition locus. Residues in red are lost-recognition; residues in green are relaxed-specificity. Regions of relevant secondary structure show χ-recognition helix, latch formed by R142 and D705, and the channel for the 3′-single-stranded DNA (ssDNA).

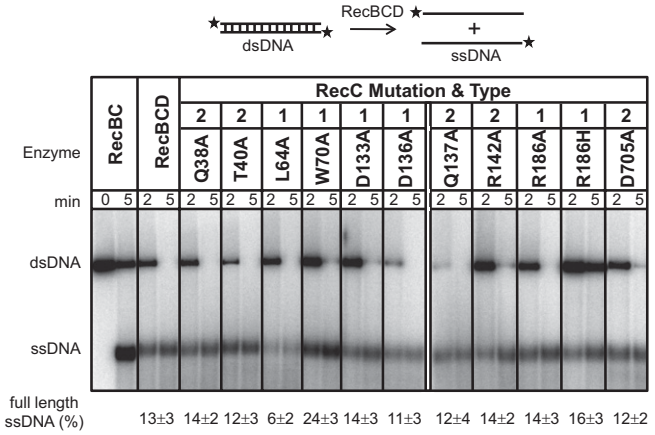


**Fig. S2.** All RecC-channel mutants retain helicase and nuclease activities that are comparable to wild-type. Time courses for dsDNA processing by RecBCD and mutant enzymes; the enzymes and reaction times are indicated. Reactions were carried out in the presence of 1 mM ATP and 2 mM $Mg(OAc)_2$, and the pBR322 dsDNA was linearized by NdeI. The positions of dsDNA and ssDNA species are indicated on the left. The final yields (± SD) of full-length ssDNA from at least three independent experiments are indicated under the gel; the normalized yield of full-length ssDNA for RecBC is 83 (±10)% and is an underestimate because of smearing of the ssDNA in the gel.

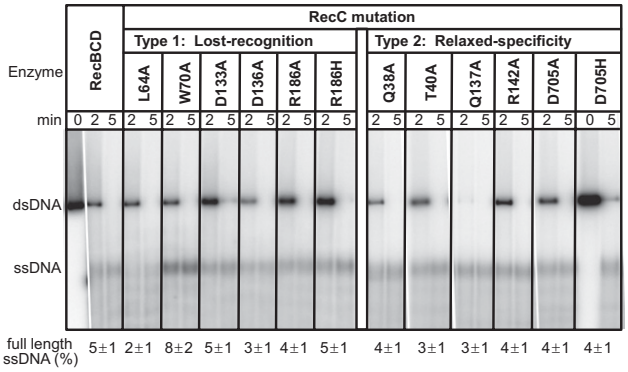


**Fig. S3.** At an elevated free $Mg^{2+}$ concentration, the RecC-channel mutants display helicase and nuclease activities that, relative to one another, are comparable. Time courses for dsDNA processing by RecBCD and mutant enzymes; the enzymes and reactions times are indicated. Reactions were carried out in the presence of 2 mM ATP and 6 mM $Mg(OAc)_2$, and the pBR322 dsDNA was linearized by NdeI. Reactions from the same gel were rearranged in the order shown. The positions of dsDNA and ssDNA species are indicated on the left. The yields (± SD) of full-length ssDNA from at least three independent experiments are indicated under the gel.

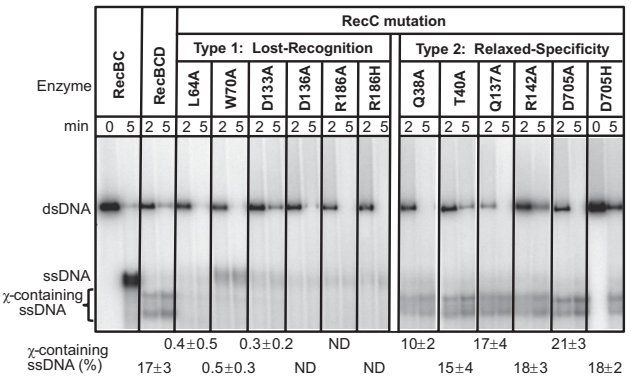


**Fig. S4.** At an elevated free $Mg^{2+}$ concentration, the type 1 (lost-recognition) mutants process dsDNA to produce substantially reduced levels of χ-specific fragments; type 2 (relaxed-specificity) mutants display wild-type level of χ recognition. The production of χ-specific fragments was carried out using $^{32}$P-labeled NdeI-linearized $\chi^3$ dsDNA in the presence of 2 mM ATP and 6 mM $Mg(OAc)_2$. The enzymes and reactions times are indicated. The positions of substrate and products are depicted on the left. The yields (± SD) of χ-containing ssDNA from at least three independent experiments are indicated under the gel; ND signifies not detectable (<0.2%).

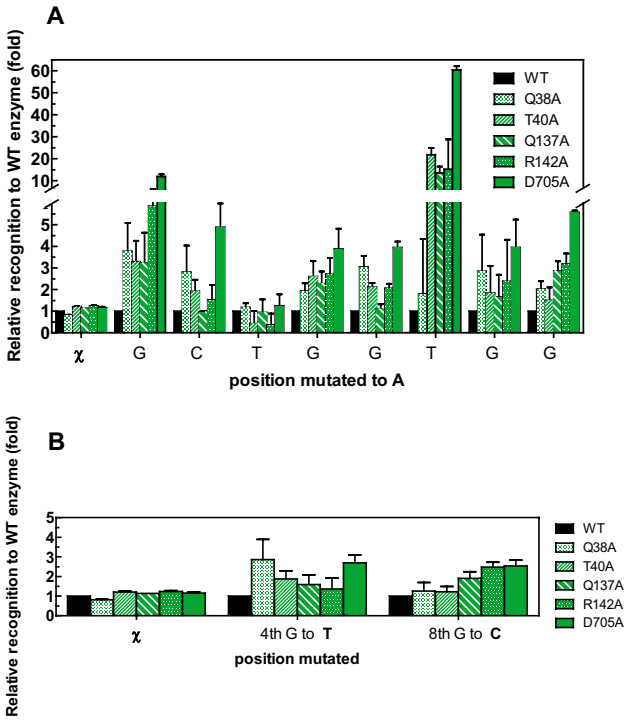


**Fig. S5.** Type 2 (relaxed-specificity) mutants recognize single-base variants of χ. The yield of variant χ-containing ssDNA produced by a mutant enzyme relative to that produced by the wild-type enzyme is plotted versus position of the canonical octameric χ sequence. Data are from Fig. 4; bars correspond to mutant enzyme described in the legend. (*A*) DNA substrates where each position of χ was replaced with an adenine residue ("A") mutation. (*B*) DNA substrates where the fourth or eighth positions of χ were replaced with thymine (T) or cytosine (C), respectively.

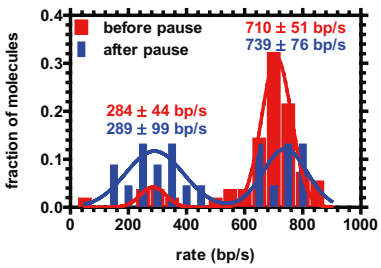


**Fig. S6.** Distribution of single-molecule translocation rates for RecBC(D705)D enzyme. The data were binned in 50-bp/s intervals and fit to the sum of two Gaussian distributions: the mean rates (± SD) for 56 molecules, before pausing, are: 284 ± 44 bp/s and 710 ± 51 bp/s; for the 23 that paused, the rates after the pause were 289 ± 99 bp/s and 739 ± 76 bp/s.

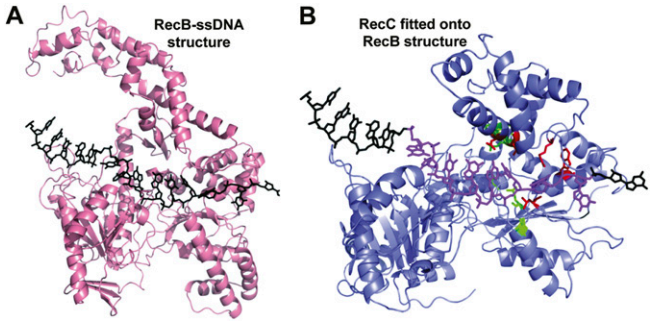


**Fig. S7.** Structural models for the interaction between χ and RecBCD (*A*) Ribbon diagram of the RecB subunit from RecBCD-DNA structure showing the location of the bound ssDNA. (*B*) Ribbon diagram of the RecC subunit with domains occupying the same positions as equivalent domains in RecB, and showing the proposed location of bound ssDNA. The eight bases in magenta are the χ sequence.

**Table S1. List of plasmids containing a variant χ sequence**

| Plasmid | Sequence |
|---|---|
| pNH92 | GCTGGTGG |
| pNH868 | **A**CTGGTGG |
| pNH869 | G**T**TGGTGG |
| pNH1556 | G**A**TGGTGG |
| pNH870 | GC**A**GGTGG |
| pNH871 | GCT**A**GTGG |
| pNH872 | GCT**T**GTGG |
| pNH873 | GCTG**A**TGG |
| pNH874 | GCTGG**A**GG |
| pNH875 | GCTGGT**A**G |
| pNH94 | GCTGGTG**C** |
| pNH95 | GCTGGTG**A** |

Boldface letters signify the variant. Plasmids pNH92, pNH94, and pNH95 were previously described (1); the others were constructed here as described in *SI Materials and Methods*.

1. Arnold DA, Handa N, Kobayashi I, Kowalczykowski SC (2000) A novel, 11 nucleotide variant of χ, χ*: One of a class of sequences defining the *Escherichia coli* recombination hotspot χ. *J Mol Biol* 300:469–479.

**Table S2. Unwinding of λ DNA by RecBCD**

| Molecule | Unwinding rate (bp/s) | Extent of unwinding (bp) |
|---|---|---|
| 1 | 374 ± 11 | 9,170 |
| 2 | 367 ± 19 | 5,830 |
| 3 | 794 ± 13 | 19,060 |
| 4 | 713 ± 10 | 27,470 |
| 5 | 286 ± 7 | 9,520 |
| 6 | 853 ± 6 | 40,480 |
| 7 | 802 ± 10 | 33,700 |
| 8 | 975 ± 16 | 16,120 |
| 9 | 854 ± 30 | 10,810 |
| 10 | 706 ± 20 | 13,040 |
| 11 | 781 ± 8 | 32,230 |
| 12 | 709 ± 26 | 11,540 |
| 13 | 584 ± 18 | 10,070 |
| 14 | 877 ± 14 | 21,430 |
| 15 | 248 ± 19 | 2,560 |
| 16 | 951 ± 8 | 34,800 |
| 17 | 883 ± 15 | 26,190 |
| 18 | 783 ± 8 | 36,630 |
| 19 | 859 ± 10 | 30,040 |
| 20 | 251 ± 12 | 7,140 |
| 21 | 794 ± 10 | 29,490 |
| 22 | 922 ± 23 | 14,410 |
| 23 | 479 ± 15 | 8,420 |
| 24 | 916 ± 8 | 37,630 |
| Mean | 368 ± 191 | 19,099 ± 868 |
| | 861 ± 99 | |

Reactions were performed in the presence of 1 mM ATP and 2 mM $Mg(OAc)_2$ at 29 °C. Unwinding rates are the best-fit values from linear regression analysis ± SE. Values for the mean rates were obtained by fitting the rate distribution to the sum of two Gaussian functions and are reported as the mean ± SD. The average extent of unwinding, *N*, is the mean ± SE.

**Table S3. Unwinding of λ DNA by RecBC(D705A)D**

| Molecule | Rate before pause (bp/s) | Pause (s) | Rate after pause (bp/s) | Position of the pause (bp) | Extent of unwinding (bp) |
|---|---|---|---|---|---|
| 1 | 714 ± 40 | 2.5 ± 2.7 | 140 ± 9 | 10,940 ± 830 | 11,560 |
| 2 | 783 ± 9 | 6.2 ± 0.5 | 784 ± 48 | 25,610 ± 420 | 28,910 |
| 3 | 724 ± 20 | 9.0 ± 0.4 | 744 ± 7 | 15,490 ± 560 | 40,080 |
| 4 | 710 ± 58 | 10.6 ± 0.6 | 658 ± 9 | 8,450 ± 890 | 28,300 |
| 5 | 849 ± 79 | 29.2 ± 0.5 | 811 ± 7 | 9,540 ± 1110 | 41,320 |
| 6 | 698 ± 104 | 4.9 ± 0.7 | 663 ± 4 | 6,880 ± 1290 | 41,030 |
| 7* | 781 ± 5 | 5.7 ± 0.9 | 260 ± 7 | 35,810 ± 340 | 42,270 |
| 8 | 727 ± 13 | 2.2 ± 0.7 | 785 ± 17 | 20,200 ± 540 | 35,310 |
| 9 | 658 ± 24 | 21.4 ± 0.7 | 238 ± 7 | 11,190 ± 520 | 15,650 |
| 10 | 769 ± 21 | 6.2 ± 0.5 | 755 ± 15 | 16,020 ± 560 | 37,620 |
| 11 | 774 ± 9 | 4.0 ± 0.6 | 705 ± 43 | 25,020 ± 420 | 29,760 |
| 12 | 304 ± 3 | 12.6 ± 1.0 | 261 ± 7 | 20,830 ± 300 | 28,910 |
| 13 | 300 ± 14 | 3.3 ± 1.1 | 741 ± 6 | 8,110 ± 540 | 41,880 |
| 14 | 687 ± 25 | 6.7 ± 0.7 | 296 ± 4 | 12,190 ± 560 | 23,580 |
| 15* | 684 ± 58 | 2.0 ± 0.9 | 327 ± 6 | 7,110 ± 780 | 17,530 |
| 16 | 247 ± 8 | 1.7 ± 1.7 | 675 ± 8 | 9,610 ± 530 | 37,970 |
| 17 | 683 ± 4 | 6.8 ± 0.7 | 460 ± 38 | 37,600 ± 340 | 38,840 |
| 18 | 269 ± 5 | 5.2 ± 0.8 | 412 ± 31 | 10,250 ± 260 | 13,800 |
| 19 | 607 ± 8 | 0.4 ± 2.0 | 323 ± 89 | 20,400 ± 590 | 21,020 |
| 20* | 740 ± 23 | 1.6 ± 1.1 | 335 ± 8 | 13,840 ± 620 | 22,190 |
| 21 | 711 ± 9 | 4.3 ± 0.1 | 219 ± 20 | 23,830 ± 340 | 23,420 |
| 22 | 774 ± 6 | 1.3 ± 1.8 | 348 ± 107 | 22,550 ± 570 | 35,770 |
| 23 | 763 ± 9 | 1.0 ± 3.2 | 172 ± 4 | 35,490 ± 750 | 41,030 |
| Mean | 284 ± 44 | 4.2 ± 0.3 | 289 ± 99 | | 23,206 ± 835 |
| | 710 ± 51 | | 739 ± 76 | | |

Reactions were performed in the presence of 1 mM ATP and 2 mM $Mg(OAc)_2$ at 29 °C. Unwinding rates before and after pausing are reported as the best fit values from three-segment line ± SE of the fitting. Values for the mean rates were obtained by fitting the rate distribution to the sum of two Gaussian functions and reported as the mean ± SD. The value for mean pause duration is the half-life time ± SE. The average extent of unwinding, *N*, was calculated from the extent of unwinding, as described in *SI Materials and Methods*, and is reported ± SE.
*Molecules depicted in Fig. 5*A*.